High-Efficiency Standby Forward Converter Integrated with DC/DC Phase-Shift Full Bridge Converter for Server Power Supply System

Shin-Young Cho, Jae-Kook Kim, Il-Woon Lee, Moon-Young Kim and Gun-Woo Moon

Department of Electrical Engineering, Guseong-dong, Yuseong-gu, Daejeon, 305-701, Korea

***Abstract* – This paper presents high-efficiency standby forward converter integrated with the DC/DC Phase-Shift Full Bridge (PSFB) converter. By sharing one leg of DC/DC PSFB converter, the proposed converter features low-voltage stress, no snubber and zero-voltage switching (ZVS) over the entire load range. Thus, the proposed converter has high-efficiency, especially under half load condition. Furthermore, by using forward-type transformer instead of flyback-type transformer in the same proposed structure, the proposed standby forward converter has low freewheeling current and higher efficiency. Experimental results of 700W prototype for server power supply system will be shown to demonstrate the feasibility of the proposed converter.**

***Index Terms*—forward, high-efficiency, integration, low voltage stress, server system, standby power, zero voltage switching.**

I. INTRODUCTION

The rate of increase in carbon dioxide emissions is accelerating. Especially, recent increasing share of carbon dioxide emissions is associated with the growth of the information communications technology (ICT) industry and global information. According to Garner's recent report on ICT industry's carbon dioxide emissions, server system is responsible for about one fourth of the total ICT industry's carbon dioxide emission since servers consume the amount of electricity for storing billions of web pages, as shown in Fig. 1 [1].

Power supplies directly consume only about 23% of total power consumption in server system. However, 60% of power consumption in server system was directly and indirectly involved in the performance of power supplies, as shown in Fig. 2 [2]. In other words, chiller and computer room air conditioner (CRAC) indirectly require more power to decrease the ambient temperature since the use of low-efficiency power supplies causes more heat to be radiated by power dissipation. Therefore, the low efficiency power supply is one of the main causes of carbon oxide emission. To improve efficiency of server power supplies, many government and organization make the some program and initiatives, such as the 80 Plus incentive program [3] and Climate Saver Computing Initiative (CSCI) [4]. The two programs require that power supplies for computer applications maintain efficiency above 80% from full load down to 20% load condition. Thus, the efficiency should be increased at the light load as well as the full load [5]. Note that, practical server power system

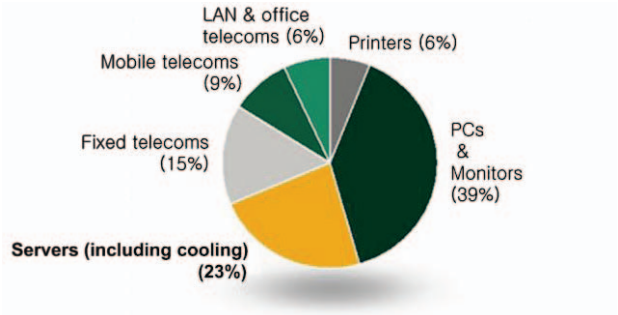

Fig. 1 Information communications technology's global carbon dioxide emissions

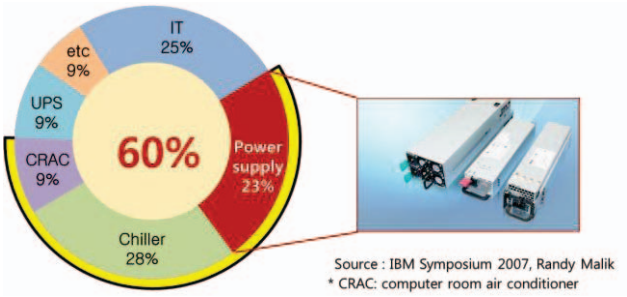

Fig. 2 Power consumption in server system

operates under half load condition most of the time so that the server power system's high-efficiency under half load condition is required [6]. Therefore the paper presents new structure to improve the efficiency, especially under half load condition.

This paper is organized as follows: the configuration, efficiency and problems of a conventional server system's power supply is shown in Section Ⅱ. And then, a general approach to use additional components and the novel approach to integrate with DC/DC PSFB is presented in Section Ⅲ and Ⅳ, respectively. To help to understand the proposed standby converter, the operational principle and analysis are explained in section Ⅴ and Ⅵ. In the following section, experimental results of 700W prototype are presented to demonstrate the feasibility of the proposed forward converter and the conclusion is drawn.

II. POWER SUPPLY FOR CONVENTIONAL SYSTEM

A. Configuration and Efficiency

Power supply for conventional server system is simply divided into three major parts: 1) PFC stage, 2) DC/DC stage and 3) standby stage. Since PFC stage and

978-1-61284-957-7/11/$26.00 ©2011 IEEE

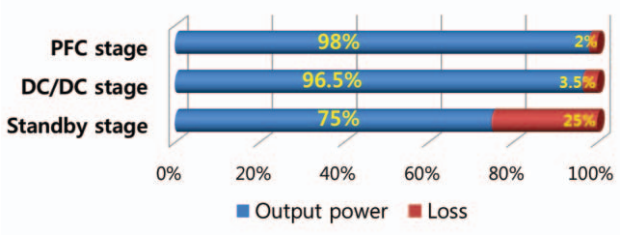

Fig. 3 Stage efficiency at half load

DC/DC stage handle most of the total power, many researches have focused on them. As a result, PFC stage and DC/DC stage have high-efficiency. However, there is a lack of research on standby stage since it deals with low power. As a result, it shows much lower efficiency than other stages, as shown in Fig 3. Therefore, this paper presents a novel high-efficiency standby converter.

B. Conventional Topology

Fig. 4 shows the DC/DC stage and standby stage of conventional system in detail. PSFB converter is one of the most widely used soft-switched topologies in DC/DC stage while flyback converter is one of the most widely used topologies in simple standby stage.

However, in conventional flyback converter for standby power, the leakage inductance L_k and the parasitic capacitor C_{oss} of the standby switch Q_A resonates after the standby switch Q_A of turned off. It results in the high-voltage stress across the standby switch Q_A due to the resonant phenomenon, as shown in Fig. 5 (a) and (b). The voltage stress of standby switch Q_A is the input voltage V_S, the reflected voltage from the secondary side NV_O and the resonance voltage across standby voltage. The voltage stress of standby switch Q_A is as follows.

$$V_{Q_{STB,\max}} = V_s + NV_o + I_{L_k,peak}\sqrt{\frac{L_k}{C_{oss}}} \quad (1)$$

Therefore, high-voltage-rated device with higher $R_{ds(on)}$ must be used. In order to have the lower voltage stress, a snubber circuit is usually adopted to deplete the leakage energy. However, snubber components can increase the conduction loss. Even so, there still exists overlarge switch voltages stress.

In addition, hard switching is another problem as the standby switch Q_A is turned on, as shown in Fig. 5 (b). Therefore, this paper proposes new high-efficiency standby converter featuring ZVS and low-voltage stress.

III. General Method of Additional Components

When some converter's disadvantages are detected, additional components are usually used to overcome the disadvantages. In this case of standby converter, a number of switches or diodes are added. For example, to overcome low-voltage converter, two-switch flyback converter (Fig. 6) could be applied. However it is considered too complex, too expensive and too bulky for,

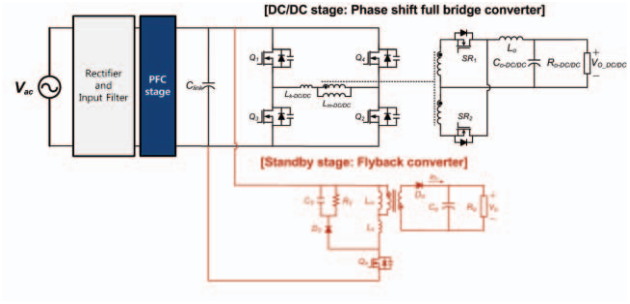

Fig. 4 DC/DC PSFB stage and standby stage of conventional system

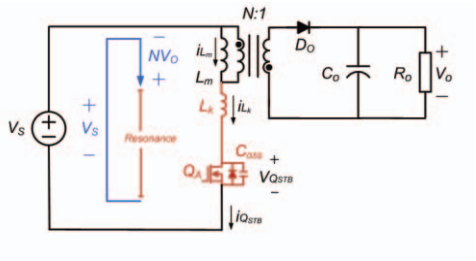

(a)

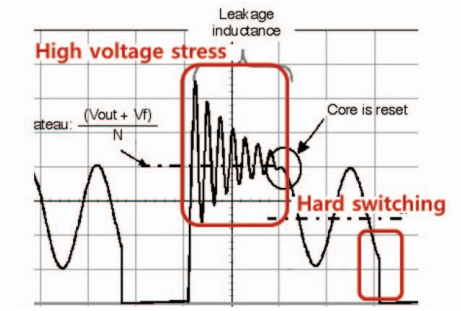

(b)

Fig. 5 Conventional converter: (a) Flyback converter without snubber, (b) Waveform

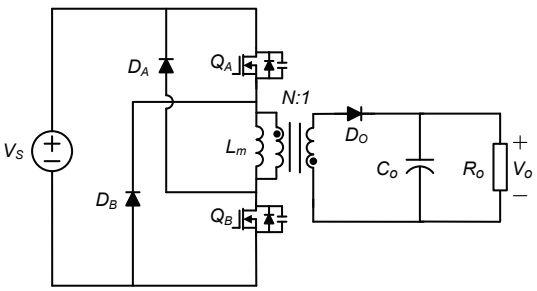

Fig. 6 Two-switch flyback converter

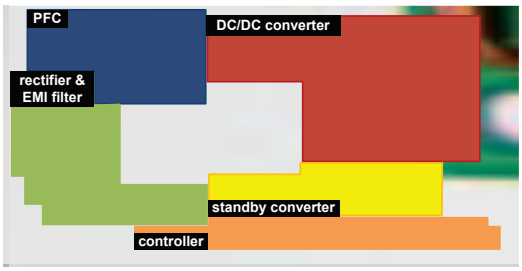

Fig. 7 Area of each stage

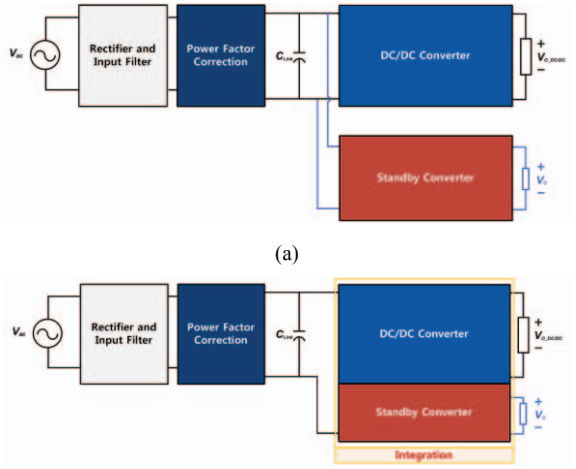

(a)

(b)

Fig. 8 Area of each stage in server power supply system: (a) conventional system (b) proposed system

standby power because of high component counts. Moreover, hard-switching problem still remain. As a result, at least more than two switches could be used for soft-switching [7], [8]. However, the use of additional components causes to increase the cost and power density. Fig 7 shows the area of each stage in server power supply. The output power of DC/DC stage is 700W and the output power of standby stage is only about 17.25W. Thus, the output power of DC/DC stage is about 40 times more than the output power of standby stage. However, the area of the DC/DC stage is only three times larger than the area of the standby stage. All things considered, the standby stage has very low power density and has no space for additional components. Therefore, using additional components is not a good solution. And the solution with no additional components is required.

IV. Proposed Method

To have no additional components, the proposed standby converter is integrated with the DC/DC PSFB converter. In conventional system, standby converter is independent with DC/DC converter, as shown in Fig. 8 (a). On the other hands, the proposed standby converter is integrated with the DC/DC converter, as shown in Fig. 8 (b). Both stages share one side leg of the bridge structure. As a result, standby stage features low component counts, clamped voltage stress of the standby converter's switch and ZVS. Therefore, the proposed converter outweighs the conventional converter in terms of efficiency, cost, and size.

A. Integration Principle

PSFB converter and two-switch flyback converter are applied for integration since the voltage stress of their switches is clamped at input voltage V_S, as shown in Fig 9 (a). After each side leg of both converters is integrated into one side leg of the proposed structure, PSFB converter still works exactly in the same way as before, and the bridge structure (the switch Q2 and Q4) help two-switch flyback converter to clamp the voltage

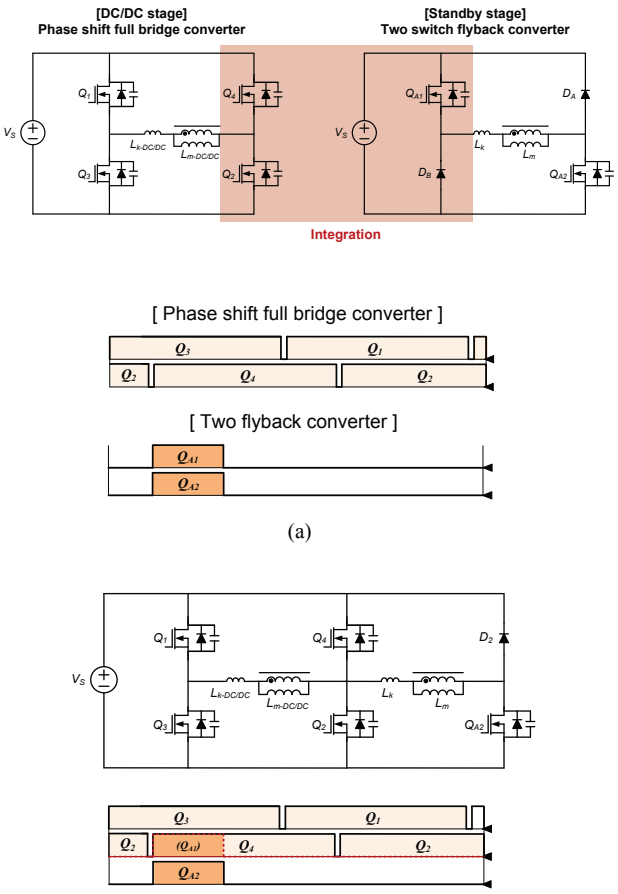

(a)

(b)

Fig. 9 Integration between DC/DC stage (PSFB converter) and standby stage (two-switch flyback converter): (a) before integration, (b) after integration

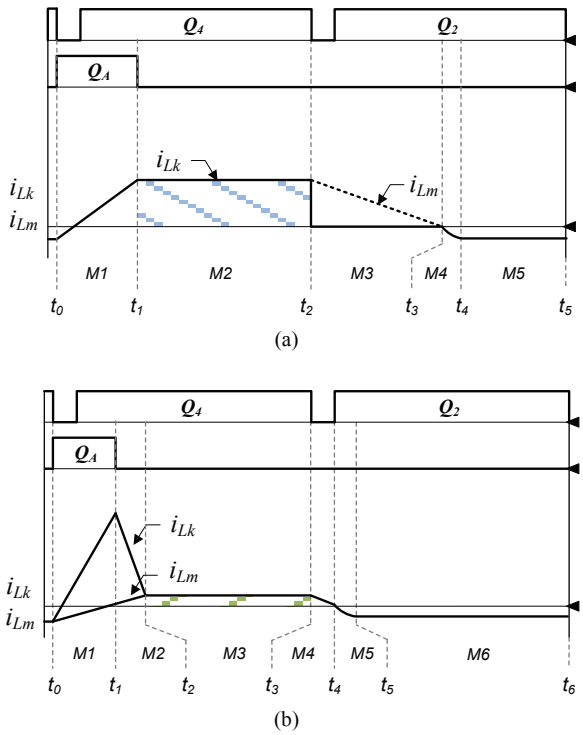

(a)

(b)

Fig. 10 the waveform of current at the primary side: (a) Flyback-type transformer (b) Forward-type transformer

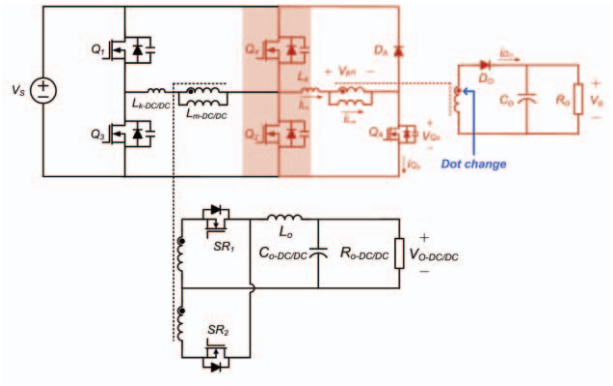

Fig. 11 Configuration of the proposed converter

.

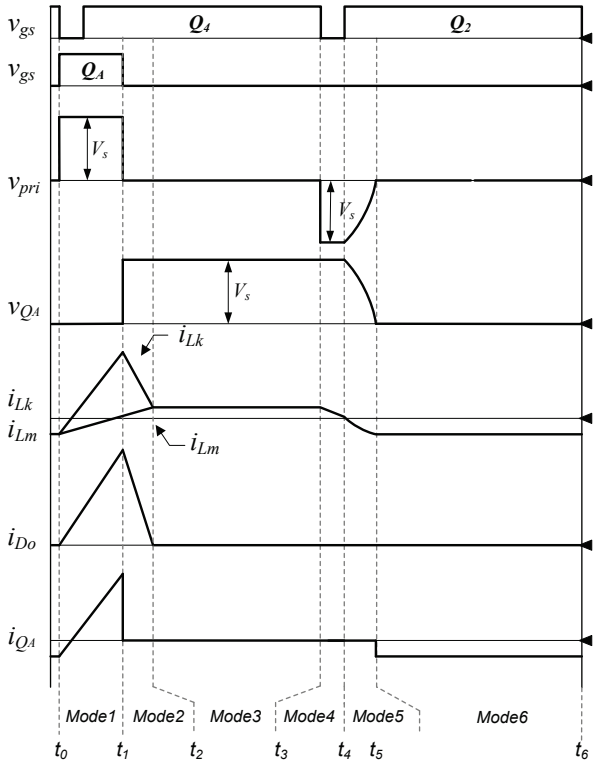

Fig. 12 Characteristic waveform of the proposed converter

stress and achieve ZVS, as shown in Fig 9 (b). The switch Q_4 operates as a switch of PSFB converter and at the same time it takes the role of the standby converter's switch Q_{A1}. And, clamping diode D_A still plays the role of reducing the voltage stress of standby switch Q_{A2} so that the voltage of standby switch Q_{A2} can be effectively clamped without snubber. Furthermore, the PSFB converter's switch Q_2 takes the role of the standby converter's diode D_B. As a result, the current of standby converter's primary side can flow in the reverse direction since a diode is changed into a switch. Therefore, the negative current leads to achieve ZVS and the proposed flyback converter has much lower switching loss than the conventional flyback converter, as discussed in more detail in Section V.

B. Forward-type Transformer

The proposed flyback converter overcomes all the conventional converter's disadvantages. Unfortunately, the proposed flyback converter causes the increase in conduction loss due to high freewheeling current, as shown from t_1 to t_2 in Fig 10 (a). However, freewheeling current can be reduced if forward-type transformer is used, as shown from t_2 to t_3 in Fig 10 (b). Note that, the forward-type converter can be designed with the higher magnetizing inductance L_m since it uses the energy stored in the leakage inductance L_k, not the magnetizing inductance L_m. Therefore, the proposed forward-type converter allows much lower freewheeling current to flow in the switch Q_4 and the clamping diodes D_A so that side effect of integration can be minimized.

V. Operational Analysis

Configuration of the proposed forward converter is shown in Fig. 11. The characteristic waveform is depicted in Fig. 12. The operational modes of the proposed forward converter can be classified into six modes in one switching cycle, as shown in Fig. 13. In order to perform the mode analysis, several assumptions are made as follows:

The transformer is modeled as a magnetizing inductor L_m, a leakage inductor L_k, and an ideal transformer with a turn ratio N (N= N_P / N_S). The input voltage Vs and the output voltage V_O are constant. And, the switches and the diodes are ideal except for their output capacitors and body diodes to simplify circuit analysis.

1) Mode 1 (t_0~t_1) [Fig. 13(a)]

Mode 1 is the powering mode. This mode begins when the gate signal of Q_A standby switch is high. At t_0, the standby switch Q_A is turned on with ZVS since the body diode was turned on before mode 1. Since the switch Q_4 and Q_A is in on-state, the primary voltage of the transformer is clamped at input voltage V_S. Then the magnetizing current i_{Lm} and leakage current i_{Lk} increases linearly. The difference between the magnetizing current i_{Lm} and leakage current i_{Lk} becomes the output current, which is scaled by the turn ratio N of the transformer. Since the diode D_O conducts and then the secondary current increase linearly, the energy stored in the primary side of the transformer is transferred to the output. This mode ends when the standby switch Q_A is turned off.

The equation of the leakage current i_{Lk} and the magnetizing current i_{Lm} are given as:

$$i_{L_k} \approx i_{L_k}(t_0) + \frac{V_s - NV_o}{L_k}(t - t_0) \tag{2}$$

$$i_{L_m} \approx i_{L_m}(t_0) + \frac{NV_o}{L_m}(t - t_0) \tag{3}$$

2) Mode 2 (t_1~t_2) [Fig. 13(b)]

Since the standby switch Q_A is turned off at t_1, the voltage of the standby switch Q_A increase up to input

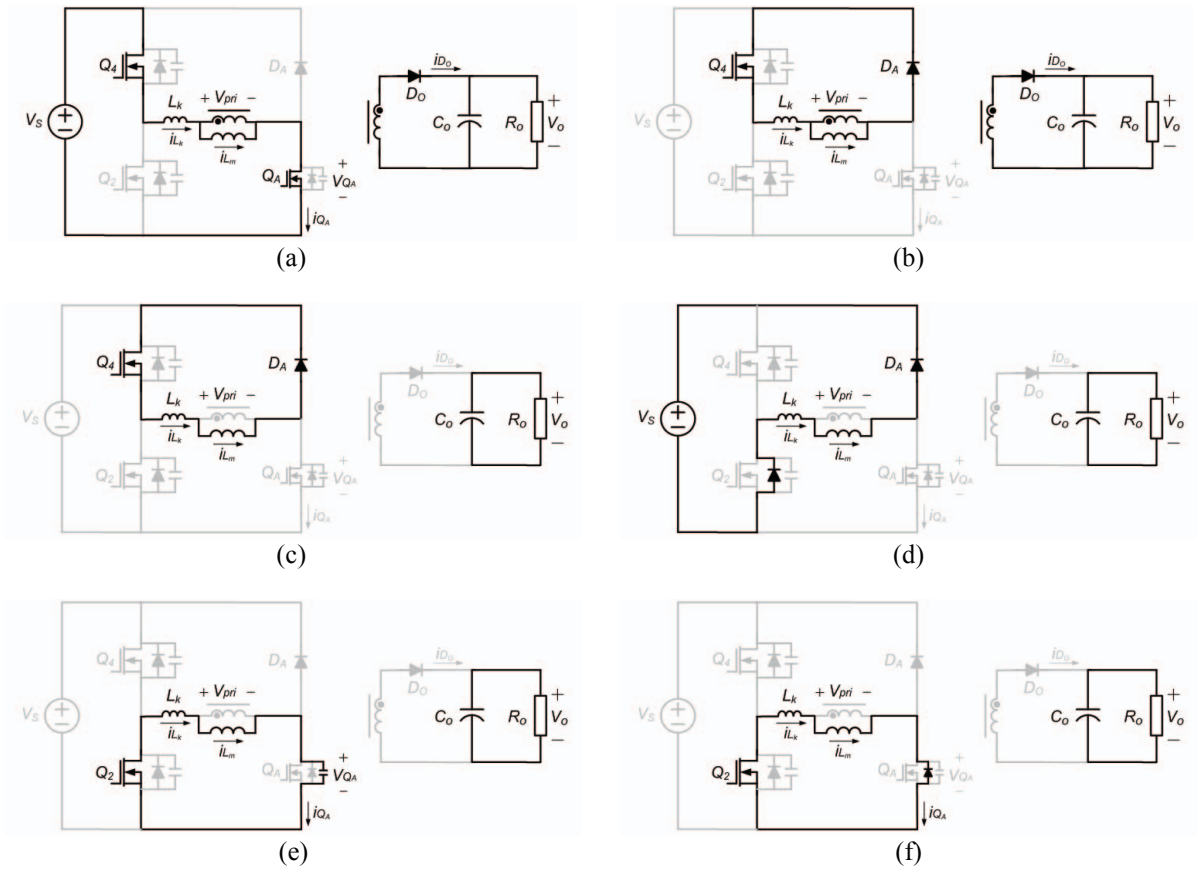

Fig. 13 Mode analysis: (a) Mode 1 [t_0-t_1], (b) Mode 2 [t_1-t_2], (c) Mode 3 [t_2-t_3], (d) Mode 4 [t_3-t_4], (e) Mode 5 [t_4-t_5], (f) Mode 6 [t_5-t_6]

voltage V_S and the primary voltage of transformer decreases to zero. And then, the primary current flows through the switch Q_4 and clamping diode D_A. At that time the leakage inductance is applied at the reflected output voltage from the secondary side, $-NV_O$ so that the leakage current i_{Lk} decreases linearly. Also, the energy stored in the primary side of the transformer is still transferred to the output. Therefore, this mode is called leakage current reset mode and powering mode. The leakage current i_{Lk} gradually decreases until the leakage current i_{Lk} meets the magnetizing current i_{Lm}. This mode and powering mode end when the leakage current i_{Lk} is equal to the magnetizing current i_{Lm}.

The equation of the leakage current i_{Lk} and the magnetizing current i_{Lm} are given as:

$$i_{L_k} \approx i_{L_k}(t_1) - \frac{NV_o}{L_k}(t - t_1) \tag{4}$$

$$i_{L_m} \approx i_{L_m}(t_1) + \frac{NV_o}{L_m}(t - t_1) \tag{5}$$

3) Mode 3 (t_2~t_3) [Fig. 13(c)]

This mode is freewheeling mode. After the leakage current i_{Lk} meets the magnetizing current i_{Lm} is turned off at t_2, the primary current continues to flows through the switch Q_4 and clamping diode D_A. The primary current is maintained constant from t_2 to t_3 so that this freewheeling current causes the increase in conduction loss. When the flyback-type transformer is used, powering is primarily related to the magnetizing inductance L_m. Therefore the value of the magnetizing inductance L_m is limited to be chosen. On the other hands, when the forward-type transformer is used, powering is less relevant to the magnetizing inductance L_m. Therefore the proposed forward-type transformer with high magnetizing inductance L_m can result in low freewheeling current. This mode ends when the switch Q_4 is turned off.

The equation of the magnetizing current i_{Lm} is given as:

$$i_{Lm} \approx i_{Lm}(t_2) \tag{6}$$

4) Mode 4 (t_3~t_4) [Fig. 13(d)]

Since the switch Q_4 is turned off at t_3, the primary voltage of transformer decreases to $-V_S$. Therefore, the magnetizing current i_{Lm} is reset since the negative voltage is applied to the primary side of the transformer.

The equation of the magnetizing current i_{Lm} is given as:

$$i_{L_m} \approx i_{L_m}(t_3) - \frac{V_s}{L_m}(t - t_3) \tag{7}$$

5) Mode 5 (t_4~t_5) [Fig. 13(e)]

This mode is resonance mode. At t_4, the magnetizing current i_{Lm} is zero. Since the magnetizing inductance L_m and the leakage inductance L_K resonate with the parasitic capacitance of the standby switch Q_A, the magnetizing current i_{Lm} changes a positive direction into a negative direction during this mode. The negative resonant current passes through the switch Q_2, and then the voltage of the standby switch Q_A resonates to zero. As a result, the body diode of the standby switch Q_A is turned on and ZVS of the standby switch Q_A is guaranteed when the standby switch Q_A is turned on.

The equation of the magnetizing current i_{Lm} is given as:

$$i_{L_m} = -\frac{V_{Q_4}(t_4)}{Z_r}\sin(\omega_r t) \tag{8}$$

$$\omega_r = \frac{1}{\sqrt{(L_m + L_k)(C_{oss})}}, Z_r = \sqrt{\frac{(L_m + L_k)}{(C_{oss})}}$$

6) Mode 6 (t_5~t_6) [Fig. 13(f)]

At the beginning of this mode t_5, the body diode of the standby switch Q_A is turned on. The primary current circulates through the switch Q_2 and the body diode of standby switch Q_A. Since the primary current still maintains negative, the standby Q_A switch can be turned on with ZVS in the next mode.

The equation of the magnetizing current i_{Lm} is given as:

$$i_{Lm} \approx i_{Lm}(t_5) \tag{9}$$

VI. Analysis Result

A. DC Conversion Ratio

The proposed forward converter operates in discontinuous conduction mode (DCM) since its DCM operation achieves the ZVS of standby switch Q_A and overcomes reverse recovery problems in the output rectifier diode D_O. In the steady-state analysis, the equation of the DC conversion ratio is as follows.

$$M = \frac{V_o}{V_s} = \frac{-N\alpha + \sqrt{N^2\alpha^2 + 4\alpha}}{2} \tag{10}$$

$$(\alpha = \frac{L_m D^2 T R_o}{2L_k(L_m + L_k)})$$

where duty cycle D is defined as the on-time ratio of the standby switch Q_A.

B. Components stress

In the proposed forward converter, the voltage stress of the standby switch Q_A is clamped to the input voltage V_S due to the clamping diode D_A of full-bridge structure. Therefore, the proposed forward converter generates no snubber loss.

C. ZVS Condition

Since standby converter operates for high-voltage/low-current application, the fixed loss at the standby switch Q_A's output capacitance occupies under load variations as follows.

$$P_{C_{oss}} = \frac{1}{2}\frac{C_{oss}V_s^2}{T_s} \tag{11}$$

The fixed loss forms a large proportion of the total loss under light load. Therefore, ZVS of the standby switch Q_A under half load condition has great influence over the standby stage's efficiency.

ZVS of the standby switch Q_A will be achieved only if the mode 4 (t_3-t_4) and the mode 5 (t_4-t_5) is less than half of the switching period T_S in Fig 10 (b). Since the mode 4 and the mode 5 constitutes a tiny fraction of the switching period T_S, the proposed forward converter achieve ZVS under entire load condition.

The equation of ZVS condition is as follows:

$$\frac{L_m}{V_s T_s}\left(\frac{V_s T_s}{L_m}\sqrt{\frac{2L_k(L_m + L_k)V_o^2}{L_m R_o(V_s^2 - NV_sV_o)T_s}} - V_s\sqrt{\frac{C_{oss}}{L_m + L_k}}\right) + \frac{\pi}{2}\sqrt{(L_m + L_k)(C_{oss})} \le \frac{T_s}{2} \tag{12}$$

Therefore, standby converter can has high efficiency due to the ZVS of standby switch Q_A.

VII. Experimental Result

To verify the operation and analysis of the proposed forward converter, three prototypes are implemented with specification of Table 1 and Table 2

TABLE I
DESIGN SPECIFICATION OF DC/DC CONVERTER

Output power	700W (12V/58A)
Switching frequency	85kHz
Device	Q_1, Q_2, Q_3 and Q_4: IPA60R250CP SR_1 and SR_2: IRFB3206

TABLE II
DESIGN SPECIFICATION OF STANDBY CONVERTER

Input voltage	320V ~ 400V	
Output power	17.25W (11.5V/1.5A)	
Core	PQ1716(PL-11)	
Inductance	Conventional flyback converter	L_m:7mH, L_k:73uH
	Proposed flyback converter	L_m:2mH, L_k:55uH
	Proposed forward converter	L_m:4.9mH, L_k:304uH
Turn	Conventional flyback converter	21:1
	Proposed flyback converter	23.5:1
	Proposed forward converter	23:1
Switch	Conventional flyback converter	Q_A:FQP5N80
	Proposed flyback converter	Q_A:FQP2N60
	Proposed forward converter	Q_A:FQP2N60
Diode	V60100CT	

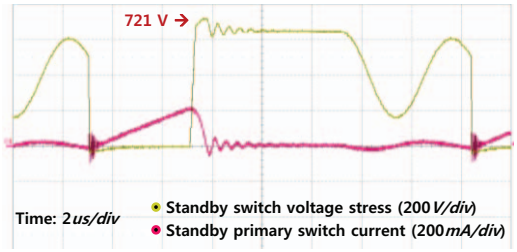

(a) Conventional flyback converter

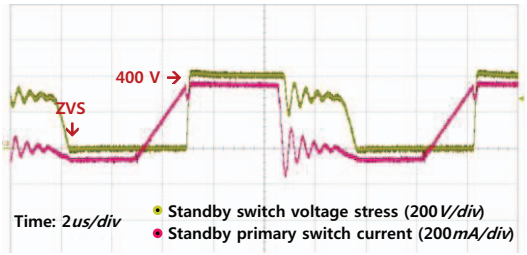

(b) Proposed flyback converter

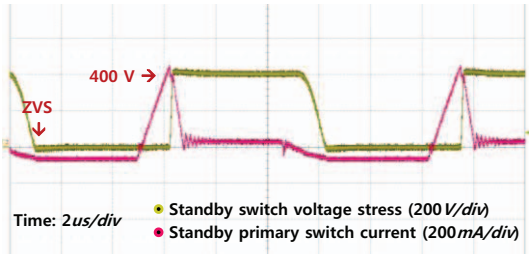

(c) Proposed forward converter

Fig. 14 Experimental waveform

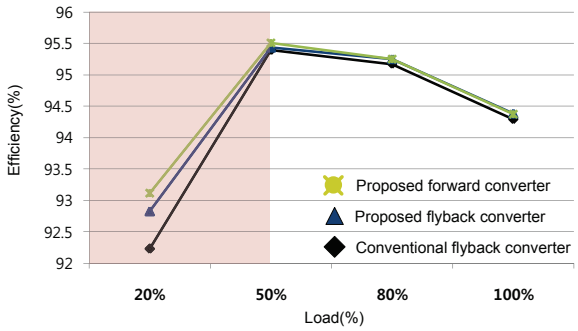

Fig. 15 Measured efficiency versus load variations

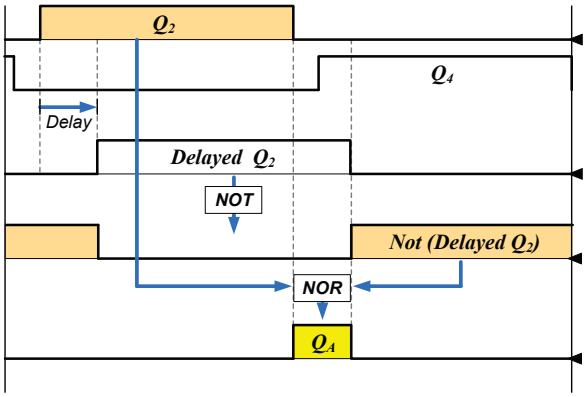

Fig. 16 Proposed converters' gate signal from gate signal of DC/DC PSFB converter

The experimental voltage and current responses of three different types of converter operating at half load condition is depicted in Fig. 14. From Fig. 14 (a), the voltage stress of standby switch Q_A is 721V. Therefore, the high-voltage-rated switch (FQP5N80) is used. Also, hard switching occurs when the standby switch Q_A is turned on. On the other hands, by observing Fig. 14 (b) and (c), the voltage of standby switch Q_A is clamped at input voltage, V_S=400V, which is much smaller than 721V. Therefore, the relatively low-voltage-rated switch (FQP2N60) is used. Moreover, the primary current keeps negative before the gate signal of standby switch is high so that both proposed converter achieve ZVS.

As can be seen from Fig. 14(b), the proposed flyback converter has high freewheeling current so that it increases the conduction loss of the switch Q_4 and clamping diode D_A substantially. However, the proposed forward converter has much lower freewheeling due to the higher magnetizing inductance L_m, as shown in Fig. 14 (c).

Fig. 15 shows measured efficiency of the conventional flyback converter, the proposed flyback converter and the proposed forward converter in normal mode. By integration, both proposed converters have higher efficiency under entire load range, especially under half load condition. This is because the proposed standby structure can achieve ZVS and eliminate snubber components and snubber loss. Since server system usually operates under half load condition, it is desirable to improve the proposed converter's efficiency under half load condition. In addition, due to low freewheeling current, the efficiency of the proposed forward converter is comparatively higher than the efficiency of the proposed flyback converter. Therefore, the proposed forward converter is the most suitable for the standby power of server power system.

VIII. Conclusion

In this paper, the high-efficiency standby converter integrated with the DC/DC PSFB converter for server power supply is presented. By the integration, the proposed forward converter has the following features. 1) A small number of devices can be used by sharing two switches with DC/DC PSPB converter. 2) High power density can be maintained due to low component counts. 3) Two proposed converters are based on the full-bridge structure so that the switch voltage stress can be clamped at the input voltage V_S and snubber loss can be eliminated. 4) The standby switch can be turned on with ZVS. 5) The conduction loss in the switch Q_4 and clamping D_A can be reduced due to high magnetizing inductance..

The validity of the basic operational principle is confirmed by the experiment. From the experimental results, the proposed forward converter has higher efficiency, especially under half load condition.

Appendix

Since both proposed converters are integrated with DC/DC PSFB converter, they operate at the same switching frequency. Therefore, gate signal for proposed

standby converter is easily derived from gate signal of DC/DC PSFB converter as shown in Fig. 16. The switch Q_2's gate signal is delayed by required duty. And then it passes through NOT-gate and becomes one input of NOR-gate. At that time, the other input of NOR-gate is the switch Q_2's gate signal. Therefore, proposed converter's gate signal is from output of NOR-gate.

REFERENCES

[1] "http://www.gartner.com/it/page.jsp?id=503867"

[2] 2008 Power and Cooling technology symposium

[3] 80 Plus Program, http://www.80plus.org/index.htm

[4] Climate Saver Computing Initiative (CSCI) Web Site, Homepage http://www.climatesaverscomputing.org. Efficiency Specification page http://www.climatesaverscomputing.org/about/faq/#4

[5] Y. Jang and M.M. Jovanovic, "A New Soft-Switched PFC Boost Rectifier with Integrated Flyback Converter for Stand-by Power." *IEEE Trans. Power Electron, vol. 21, no.1, pp66-72, Jan. 2006.*

[6] 2008 Power and Cooling technology symposium.

[7] Jinbin Zhao, Fengzhi Dai, "Soft-Switching Two-Switch Flyback Converter With Wide Range" *Industrial Electronics and Applications, 2008. ICIEA 2008. 3rd IEEE Conf. 2008.pp. 250-254*

[8] Wang. C.M, Su. C.M and Yang. C.H "ZVS-PWM flyback converter with a simple auxiliary" *IEEE Trans. Power Electron, vol. 153, no.1, pp116, Jan. 2006*